PAPER

NJC
www.rsc.org/njc

A series of new polyoxoanion-based inorganic-organic hybrids: $(C_6NO_2H_5)[(H_2O)_4(C_6NO_2H_5)Ln(CrMo_6H_6O_{24})]\cdot 4H_2O$ (Ln = Ce, Pr, La and Nd) with a chiral layer structure†

Haiyan An, Dongrong Xiao, Enbo Wang,* Yangguang Li and Lin Xu

Institute of Polyoxometalate Chemistry, Department of Chemistry, Northeast Normal University, Changchun, 130024, P. R. China. E-mail: wangenbo@public.cc.jl.cn

Received (in Montpellier, France) 16th November 2004, Accepted 27th January 2005
First published as an Advance Article on the web 13th April 2005

Four new polyoxoanion-based hybrids with a chiral layer structure, $(C_6NO_2H_5)[(H_2O)_4(C_6NO_2H_5)Ln(CrMo_6H_6O_{24})]\cdot 4H_2O$ (Ln = Ce, **1**; Pr, **2**; La, **3** and Nd, **4**), have been synthesized and characterized by elemental analysis, IR spectroscopy, TG analysis and single crystal X-ray diffraction. All the compounds are isostructural and crystallize in the monoclinic space group *C*2/*c*. Their crystal structures consist of two kinds of chiral layers, one left-handed and the other right-handed, each built up from the same-handed rare earth polyoxometalate helical chains, which leads to mesomeric solid state compounds. To our knowledge, this represents the first example of a 2D chiral layer framework consisting of rare earth polyoxometalate helical chains and organic bridging ligands. The magnetic properties of compounds **1**, **2** and **4** have been studied by measuring their magnetic susceptibility over the temperature range of 2–300 K.

Introduction

Current interest in the crystal engineering of inorganic-organic hybrid materials not only stems from their special applications in catalysis, sorption, biology, and as optical and electromagnetic functional materials, but also from their intriguing variety of architectures and topologies.[1,2] In the vast amount of reported work, the rational synthesis of inorganic-organic compounds containing helical or chiral structures is of particular interest.[3] Up to now, a variety of helical coordination polymers through the self-assembly of ligands and metal cations have been reported.[4,5] In contrast, only a few hybrid compounds containing polyoxoanions and organic ligands and/or metal coordination complexes are reported to possess helical character, although they have become an important class of inorganic-organic materials owing to their fascinating properties and potential applications in a wide number of fields. For instance, double helical chains have been described in vanadium phosphates, $[(CH_3)_2NH_2]K_4[V_{10}O_{10}(H_2O)_2(OH)_4(PO_4)_7]$[6] and $[M(4,4'\text{-bpy})_2(VO_2)_2(HPO_4)_4]$,[7] intersecting helical channels in an open-framework zinc phosphate, $[NH_3(CH_2)_2NH_2(CH_2)_2NH_3][Zn_4(PO_4)_3(HPO_4)]H_2O$,[8] and a new helical chain constructed from molybdenum oxide in $[NH_3(CH_2)_2NH_2(CH_2)_2NH_3]_2[Mo_9O_{30}]$.[9] Therefore, the exploration of suitable polyoxoanion building units and structure-directing agents to construct hybrid frameworks with helical or chiral character is one of the most challenging issues in current synthetic chemistry and materials science.

It should be noted that polyoxometalates (POMs),[10,11] an important class of polyoxoanion clusters, have been employed for the construction of interesting 1D chain, 2D layer, and even 3D inorganic-organic hybrid compounds, which have been thoroughly reviewed by Zubieta and co-workers.[12] In comparison to the large number of hybrid polyoxoanion-based solid materials structurally modified by 3d-block transition metal complexes,[13,14] lanthanide coordination complexes as inorganic bridging linkers have received far less attention,[15] although they may possess interesting spectroscopic and magnetic properties.[16] On the other hand, while recently we, and others, have reported a few 1D chain-like polymers constructed from Anderson-type polyoxoanion clusters with lanthanide ions as linkers,[17,18] higher dimensional inorganic-organic hybrid compounds based on this type of polyoxoanion remain largely unreported.[19] Hence, our current synthetic strategy is to acquire new high-dimensional inorganic-organic hybrid compounds containing helical or chiral structures, constructed from Anderson-type polyoxoanions and lanthanide-organic coordination complexes as linkers, based on the following considerations: (i) the high reactivity of this kind of polyoxoanion makes possible the formation of high-dimensional extended structures; (ii) the lability of terminal water molecules in lanthanide centers linked to polyoxoanions opens the way to the design of extended hybrid frameworks through replacing water molecules by bidentate organic ligands; (iii) organic molecules can dramatically influence the inorganic oxide microstructure.[3d,6,7,9,20] We describe in this paper a series of novel 2D polyoxoanion-based hybrid compounds, $(C_6NO_2H_5)[(H_2O)_4(C_6NO_2H_5)Ln(CrMo_6H_6O_{24})]\cdot 4H_2O$ (Ln = Ce **1**, Pr **2**, La **3** and Nd **4**), containing chiral layer structures. Each compound consists of two kinds of chiral layers, one right-handed and one left-handed, leading to a mesomeric compound. Interestingly, each 2D chiral layer is built up from the same-handed rare earth POM helical chains that are linked up together by organic ligands. This represents the first example of a 2D chiral layer framework consisting of rare earth POM helical chains and organic bridging ligands.

Experimental

Materials and measurements

$PrCl_3$ and $NdCl_3$ were prepared by dissolving the corresponding oxides in dilute hydrochloric acid and then heating to

† Electronic supplementary information (ESI) available: Additional structural views and information on compounds **1–4**; IR spectra and TGA graphs of compounds **1–4**. See http://www.rsc.org/suppdata/nj/b4/b417313a/

DOI: 10.1039/b417313a

Table 1 Crystal data and structure refinement for **1**, **2**, **3** and **4**

Complex	**1**	**2**	**3**	**4**
Formula	$C_{12}H_{32}N_2CeCrMo_6O_{36}$	$C_{12}H_{32}N_2PrCrMo_6O_{36}$	$C_{12}H_{32}N_2LaCrMo_6O_{36}$	$C_{12}H_{32}N_2NdCrMo_6O_{36}$
Formula weight	1548.16	1548.95	1546.95	1552.28
T/K	293(2)	293(2)	293(2)	293(2)
λ/Å	0.71073	0.71073	0.71073	0.71073
Crystal system	Monoclinic	Monoclinic	Monoclinic	Monoclinic
Space group	$C2/c$	$C2/c$	$C2/c$	$C2/c$
a/Å	23.616(5)	23.624(5)	23.772(5)	23.564(5)
b/Å	13.384(3)	13.366(3)	13.440(3)	13.388(3)
c/Å	24.746(5)	24.727(5)	24.754(5)	24.787(5)
β/Å	103.06(3)	103.06(3)	103.10(3)	103.00(3)
U/Å^3	7619(3)	7606(3)	7703(3)	7619(3)
Z	8	8	8	8
μ/mm^{-1}	3.470	3.560	3.360	3.638
Total reflections	36691	35737	35741	25678
Indep. reflections	8720	8702	8743	7936
R_{int}	0.0479	0.0986	0.1207	0.1090
$R1$ [$I > 2\sigma(I)$]	0.0286	0.0543	0.0557	0.0698
$wR2$ [$I > 2\sigma(I)$]	0.0629	0.1295	0.1152	0.1700
$R1$ (all data)	0.0384	0.0822	0.0989	0.1185
$wR2$ (all data)	0.0665	0.1448	0.1348	0.2033

dryness. $Na_3[CrMo_6H_6O_{24}]\cdot 8H_2O$ was synthesized according to the literature and characterized by IR spectroscopy and TG analysis.[21] All the other chemicals were purchased from commercial sources and used without further purification. Elemental analyses (C, H, and N) were performed on a Perkin–Elmer 2400 CHN elemental analyzer; Cr, Mo, Ce, Pr, La and Nd were analyzed on a Plasma-Spec(I) ICP atomic emission spectrometer. IR spectra were recorded in the range 400–4000 cm^{-1} on an Alpha Centaur FT/IR spectrophotometer using KBr pellets. TG analyses were performed on a Perkin–Elmer TGA7 instrument in flowing N_2 with a heating rate of 10 °C min^{-1}. Variable-temperature magnetic susceptibility data were obtained on a SQUID magnetometer (Quantum Design, MPMS-7) in the temperature range of 2–300 K with an applied field of 1 T. Samples for the magnetic measurements were ground into powder in order to avoid anisotropy effects.[22a] Corrections were applied for diamagnetism using Pascal's constants[22b] and for the sample holders.

Synthesis

$(C_6NO_2H_5)[(H_2O)_4(C_6NO_2H_5)Ln(CrMo_6H_6O_{24})]\cdot 4H_2O$ (1–4). In a typical experiment, pyridine-4-carboxylic acid (0.246 g, 2 mmol) and $Ce(NO_3)_3\cdot 6H_2O$ (0.434 g, 1 mmol) were dissolved in 20 ml of hot water. Then, 20 ml of a water solution of $Na_3[CrMo_6H_6O_{24}]\cdot 8H_2O$ (1.231 g, 1 mmol) was added. The initial pH of the mixture was 2.95. The mixture was refluxed for 2 h at 80 °C, then filtered. The filtrate was kept for one month under ambient conditions, after which time yellow block crystals of **1** were isolated in about 40% yield (based on Ce). Anal. calcd for $(C_6NO_2H_5)[(H_2O)_4(C_6NO_2H_5)Ce(CrMo_6H_6O_{24})]\cdot 4H_2O$: Cr, 3.36; Mo, 37.18; Ce, 9.05; C, 9.31; H, 2.07; N, 1.81 (%); found: Cr, 3.21; Mo, 36.71; Ce, 9.30; C 9.40; H, 1.87; N, 1.95 (%); FTIR (cm^{-1}): 3614 (w), 3409 (m), 1638 (m), 1590 (s), 1578 (s), 1398 (m), 1244 (w), 1153 (w), 1058 (w), 1004 (w), 939 (s), 897 (s), 853 (m), 770 (m), 642 (vs), 566 (w) and 410 (m).

2: $PrCl_3$; pink crystals; 45% yield; anal. calcd for $(C_6NO_2H_5)[(H_2O)_4(C_6NO_2H_5)Pr(CrMo_6H_6O_{24})]\cdot 4H_2O$ Cr, 3.36; Mo, 37.16; Pr, 9.10; C, 9.30; H, 2.07; N, 1.81 (%); found: Cr, 3.15; Mo, 36.71; Pr, 9.32; C 9.47; H, 2.35; N, 1.65 (%); FTIR (cm^{-1}): 3614 (w), 3409 (m), 1637 (m), 1591 (s), 1577 (s), 1398 (m), 1244 (w), 939 (s), 897 (s), 853 (m), 770 (m), 642 (vs), 566 (w) and 410 (m).

3: $La(NO_3)_3\cdot 6H_2O$; pink crystals; 35% yield; anal. calcd for $(C_6NO_2H_5)[(H_2O)_4(C_6NO_2H_5)La(CrMo_6H_6O_{24})]\cdot 4H_2O$ Cr, 3.36; Mo, 37.21; La, 8.98; C, 9.32; H, 2.07; N, 1.81 (%); found: Cr, 3.20; Mo, 36.83; La, 9.12; C 9.57; H, 2.35; N, 1.68 (%); FTIR (cm^{-1}): 3616 (w), 3153 (m), 3089 (m), 1638 (m), 1591 (s), 1577 (s), 1398 (m), 1244 (w), 939 (s), 896 (s), 853 (m), 770 (m), 642 (vs), 566 (w) and 410 (m).

4: $NdCl_3$; pink crystals; 37% yield; anal. calcd for $(C_6NO_2H_5)[(H_2O)_4(C_6NO_2H_5)Nd(CrMo_6H_6O_{24})]\cdot 4H_2O$ Cr, 3.35; Mo, 37.08; Nd, 9.29; C, 9.28; H, 2.06; N, 1.80 (%); found: Cr, 3.18; Mo, 37.22; Nd, 9.44; C 9.01; H, 2.37; N, 1.68 (%); FTIR (cm^{-1}): 3613 (w), 3156 (m), 3089 (m), 1639 (m), 1592 (s), 1577 (s), 1398 (m), 1244 (w), 939 (s), 897 (s), 853 (m), 770 (m), 643 (vs), 566 (w) and 413 (m).

X-Ray crystallography

Suitable single crystals with dimensions of 0.35 × 0.31 × 0.28 mm for **1**, 0.26 × 0.25 × 0.18 mm for **2**, 0.28 × 0.26 × 0.18 mm for **3** and 0.22 × 0.20 × 0.14 mm for **4** were selected for single-crystal X-ray diffraction analysis. Empirical absorption correction was applied. The structures of **1–4** were solved by direct methods and refined by full-matrix least squares on F^2 using the SHELXTL-97 software.[23] All of the non-hydrogen atoms were refined anisotropically except for OW7, OW8 and OW9 in **1**, OW8 and OW9 in **2**, and O4, C3, C6, C10, OW7, OW8 and OW9 in **4**. In **1**, positions of the hydrogen atoms attached to polyoxoanions were located from difference maps. The hydrogen atoms attached to nitrogen atoms were located from difference maps and those attached to carbon atoms were fixed in ideal positions in **1**. The hydrogen atoms attached to water molecules, except for OW7, OW8 and OW9, were located from difference maps, and those attached to free OW7, OW8 and OW9 were not located in **1**. In **2**, **3** and **4** positions of the hydrogen atoms attached to carbon atoms and those attached to nitrogen atoms were fixed in ideal positions; other hydrogen atoms were not located.

Results and discussion

Description of the crystal structures

Single crystal X-ray diffraction analyses revealed that compounds **1–4** are isostructural and the unit cell dimensions, volumes, related bond distances and angles vary only slightly (Tables 1–5).‡ The structure of the four composite compounds

‡ CCDC reference numbers: 255009 for **1**, 255011 for **2**, 255010 for **3** and 255389 for **4**. See http://www.rsc.org/suppdata/nj/b4/b417313a/ for crystallographic data in .cif or other electronic format.

Table 2 Selected bond lengths (Å) and angles (°) for **1**[a]

Cr(1)–O(1)	1.958(3)	Mo(3)–O(3)	2.284(3)
Cr(1)–O(6)	1.972(3)	Mo(3)–O(18)	1.706(3)
Cr(1)–O(4)	1.986(3)	Mo(3)–O(17)	1.719(3)
Cr(1)–O(5)	1.967(3)	Mo(3)–O(9)	1.928(3)
Cr(1)–O(2)	1.972(3)	Mo(3)–O(8)	1.933(3)
Cr(1)–O(3)	1.972(3)	Mo(4)–O(19)	1.705(3)
Mo(1)–O(14)	1.682(3)	Mo(4)–O(9)	1.984(3)
Mo(1)–O(13)	1.740(3)	Mo(4)–O(4)	2.280(3)
Mo(1)–O(7)	1.905(3)	Mo(5)–O(21)	1.700(3)
Mo(1)–O(12)	1.950(3)	Mo(5)–O(10)	1.966(3)
Mo(1)–O(6)	2.261(3)	Mo(5)–O(5)	2.292(3)
Mo(1)–O(1)	2.323(3)	Mo(6)–O(23)	1.713(3)
Mo(2)–O(16)	1.700(3)	Mo(6)–O(12)	1.918(3)
Mo(2)–O(15)	1.712(3)	Mo(6)–O(6)	2.330(3)
Mo(2)–O(8)	1.944(3)	Ce(1)–O(13)	2.442(3)
Mo(2)–O(7)	1.944(3)	Ce(1)–O(25)	2.526(3)
Mo(2)–O(1)	2.241(3)	Ce(1)–O(26)#1	2.536(3)
Mo(2)–O(2)	2.311(3)	Ce(1)–O(17)#2	2.537(3)
Mo(3)–O(2)	2.263(3)	Ce(1)–O(25)#1	2.726(3)
O(1)–Cr(1)–O(5)	94.00(11)	O(16)–Mo(2)–O(15)	105.60(17)
O(1)–Cr(1)–O(2)	84.54(11)	O(16)–Mo(2)–O(8)	99.93(13)
O(2)–Cr(1)–O(4)	98.10(11)	O(14)–Mo(1)–O(13)	104.88(15)
O(5)–Cr(1)–O(2)	178.52(12)	O(14)–Mo(1)–O(7)	101.97(13)
O(5)–Cr(1)–O(4)	83.37(11)	O(26)#1–Ce(1)–O(17)#2	71.98(10)
O(3)–Cr(1)–O(6)	178.41(12)	O(13)–Ce(1)–O(25)	84.58(10)

[a] Symmetry transformations used to generate equivalent atoms: #1 $-x$, y, $-z+21/2$, #2 $-x+1/2$, $y+1/2$, $-z+1/2$.

Table 4 Selected bond lengths (Å) and angles (°) for **3**[a]

Cr(1)–O(4)	1.965(6)	Mo(3)–O(17)	1.682(7)
Cr(1)–O(6)	1.970(6)	Mo(3)–O(18)	1.705(7)
Cr(1)–O(2)	1.974(6)	Mo(3)–O(8)	1.949(6)
Cr(1)–O(5)	1.976(6)	Mo(3)–O(9)	1.973(7)
Cr(1)–O(1)	1.983(6)	Mo(3)–O(3)	2.292(6)
Cr(1)–O(3)	2.000(6)	Mo(3)–O(2)	2.301(6)
Mo(1)–O(14)	1.689(6)	Mo(4)–O(9)	1.902(7)
Mo(1)–O(13)	1.735(6)	Mo(4)–O(4)	2.291(6)
Mo(1)–O(12)	1.896(6)	Mo(5)–O(22)	1.712(6)
Mo(1)–O(7)	1.952(6)	Mo(5)–O(4)	2.290(6)
Mo(1)–O(1)	2.261(6)	Mo(6)–O(23)	1.690(7)
Mo(1)–O(6)	2.337(6)	Mo(6)–O(11)	1.944(6)
Mo(2)–O(16)	1.715(6)	Mo(6)–O(5)	2.318(6)
Mo(2)–O(15)	1.727(6)	La(1)–O(13)	2.470(6)
Mo(2)–O(7)	1.927(6)	La(1)–O(26)#1	2.552(6)
Mo(2)–O(8)	1.941(6)	La(1)–O(22)#2	2.567(6)
Mo(2)–O(2)	2.248(6)	La(1)–O(25)	2.572(7)
Mo(2)–O(1)	2.335(6)	La(1)–O(26)	2.739(6)
O(4)–Cr(1)–O(1)	178.4(3)	O(13)–La(1)–O(26)#1	84.6(2)
O(6)–Cr(1)–O(1)	84.3(2)	OW3–La(1)–O(22)#2	144.7(2)
O(2)–Cr(1)–O(3)	83.4(2)	O(14)–Mo(1)–O(13)	104.2(3)
O(5)–Cr(1)–O(3)	98.1(2)	O(15)–Mo(2)–O(8)	96.8(3)
O(6)–Cr(1)–O(2)	93.7(2)	O(7)–Mo(2)–O(8)	148.4(3)
O(4)–Cr(1)–O(5)	84.7(2)	O(14)–Mo(1)–O(13)	104.2(3)

[a] Symmetry transformations used to generate equivalent atoms: #1 $-x$, y, $-z+1/2$, #2 $-x+1/2$, $y+1/2$, $-z+1/2$.

exhibits an unusual 2D layer framework composed of $[Cr(OH)_6Mo_6O_{18}]^{3-}$ polyoxoanion clusters, Ln(pyridine-4-carboxylic acid) coordination complexes (Ln = Ce **1**, Pr **2**, La **3** and Nd **4**), free pyridine-4-carboxylic acid molecules and lattice water molecules. The $[Cr(OH)_6Mo_6O_{18}]^{3-}$ cluster has a B-type Anderson structure, which is made up of seven edge-sharing octahedra, six of which are $\{MoO_6\}$ octahedra arranged hexagonally around the central $\{Cr(OH)_6\}$ octahedron (see Fig. 1 and Fig. S2 in the Electronic supplementary information, ESI).

Selected bond lengths and angles of **1–4** are listed in Tables 2–5, respectively (see additional data in Table S1 in the ESI). Four kinds of oxygen atoms exist in the cluster according to the way the oxygen atoms are coordinated: terminal oxygen Ot, terminal oxygen Ot′ linked to Ln^{3+}, double-bridging oxygen Ob, and central oxygen Oc. Thus the Mo–O distances can be grouped into four sets: Mo–Ot 1.682–1.713, Mo–Ot′ 1.719–1.740, Mo–Ob 1.905–1.984 and Mo–Oc 2.241–2.330 Å in **1**; Mo–Ot 1.681–1.723, Mo–Ot′ 1.722, Mo–Ob 1.898–1.988

Table 3 Selected bond lengths (Å) and angles (°) for **2**[a]

Cr(1)–O(4)	1.965(6)	Mo(3)–O(17)	1.692(7)
Cr(1)–O(6)	1.966(5)	Mo(3)–O(8)	1.935(6)
Cr(1)–O(2)	1.970(6)	Mo(3)–O(9)	1.973(7)
Cr(1)–O(5)	1.972(6)	Mo(3)–O(3)	2.286(6)
Cr(1)–O(1)	1.977(6)	Mo(3)–O(2)	2.303(5)
Cr(1)–O(3)	1.994(5)	Mo(4)–O(9)	1.898(6)
Mo(1)–O(14)	1.681(7)	Mo(4)–O(10)	1.988(6)
Mo(1)–O(13)	1.722(6)	Mo(4)–O(3)	2.281(6)
Mo(1)–O(12)	1.909(5)	Mo(5)–O(4)	2.291(5)
Mo(1)–O(7)	1.934(6)	Mo(5)–O(22)	1.722(6)
Mo(1)–O(1)	2.261(5)	Mo(5)–O(11)	1.937(6)
Mo(1)–O(6)	2.325(6)	Mo(6)–O(24)	1.710(6)
Mo(2)–O(16)	1.704(6)	Mo(6)–O(11)	1.944(6)
Mo(2)–O(15)	1.723(6)	Mo(6)–O(6)	2.248(6)
Mo(2)–O(7)	1.924(5)	Pr(1)–O(25)#2	2.710(6)
Mo(2)–O(8)	1.951(5)	Pr(1)–O(13)	2.449(6)
Mo(2)–O(2)	2.251(6)	Pr(1)–O(22)#1	2.525(6)
Mo(2)–O(1)	2.331(5)	Pr(1)–O(25)	2.525(7)
Mo(3)–O(18)	1.682(6)	Pr(1)–O(26)#2	2.526(6)
O(4)–Cr(1)–O(2)	95.5(2)	OW4–Pr(1)–O(13)	83.2(2)
O(6)–Cr(1)–O(5)	84.9(2)	O(13)–Pr(1)–O(22)#1	138.0(2)
O(4)–Cr(1)–O(1)	178.5(2)	O(14)–Mo(1)–O(13)	105.3(3)
O(2)–Cr(1)–O(1)	84.8(2)	O(14)–Mo(1)–O(12)	101.8(3)
O(5)–Cr(1)–O(1)	94.8(2)	O(16)–Mo(2)–O(15)	106.2(3)
O(4)–Cr(1)–O(3)	83.3(2)	O(16)–Mo(2)–O(7)	99.9(3)

[a] Symmetry transformations used to generate equivalent atoms: #1 $-x+1/2$, $y-1/2$,$-z+1/2$, #2 $-x$, y, $-z+1/2$.

Table 5 Selected bond lengths (Å) and angles (°) for **4**[a]

Cr(1)–O(3)	1.957(8)	Mo(3)–O(18)	1.696(9)
Cr(1)–O(5)	1.963(8)	Mo(3)–O(17)	1.732(9)
Cr(1)–O(1)	1.976(9)	Mo(3)–O(9)	1.918(9)
Cr(1)–O(6)	1.985(8)	Mo(3)–O(8)	1.934(9)
Cr(1)–O(2)	1.989(9)	Mo(3)–O(2)	2.256(9)
Cr(1)–O(4)	1.997(9)	Mo(3)–O(3)	2.299(8)
Mo(1)–O(14)	1.686(9)	Mo(4)–O(10)	1.894(9)
Mo(1)–O(13)	1.744(9)	Mo(4)–O(9)	1.997(8)
Mo(1)–O(7)	1.914(8)	Mo(4)–O(3)	2.305(9)
Mo(1)–O(12)	1.959(9)	Mo(5)–O(21)	1.678(10)
Mo(1)–O(6)	2.273(8)	Mo(5)–O(22)	1.711(9)
Mo(1)–O(1)	2.324(8)	Mo(5)–O(10)	1.979(9)
Mo(2)–O(15)	1.698(9)	Mo(6)–O(24)	1.724(9)
Mo(2)–O(16)	1.705(11)	Mo(6)–O(12)	1.914(9)
Mo(2)–O(8)	1.950(9)	Mo(6)–O(6)	2.325(8)
Mo(2)–O(7)	1.958(8)	Nd(1)–O(13)	2.417(9)
Mo(2)–O(1)	2.241(9)	Nd(1)–O(26)#1	2.497(9)
Mo(2)–O(2)	2.314(10)	Nd(1)–O(17)#2	2.506(8)
Nd(1)–O(25)#1	2.698(10)	Nd(1)–O(25)	2.511(9)
O(3)–Cr(1)–O(5)	95.7(4)	O(13)–Mo(1)–O(6)	161.0(4)
O(3)–Cr(1)–O(2)	84.4(3)	O(7)–Mo(1)–O(1)	71.2(3)
O(5)–Cr(1)–O(2)	178.2(4)	O(16)–Mo(2)–O(2)	161.1(4)
O(5)–Cr(1)–O(4)	84.2(3)	O(8)–Mo(2)–O(2)	70.8(3)
O(6)–Cr(1)–O(2)	95.1(3)	O(13)–Nd(1)–OW1	82.9(3)
O(3)–Cr(1)–O(6)	177.9(4)	O(13)–Nd(1)–O(17)#2	137.6(3)

[a] Symmetry transformations used to generate equivalent atoms: #1 $-x+1$, y, $-z-1/2$, #2 $-x+1/2$, $y+1/2$, $-z-1/2$.

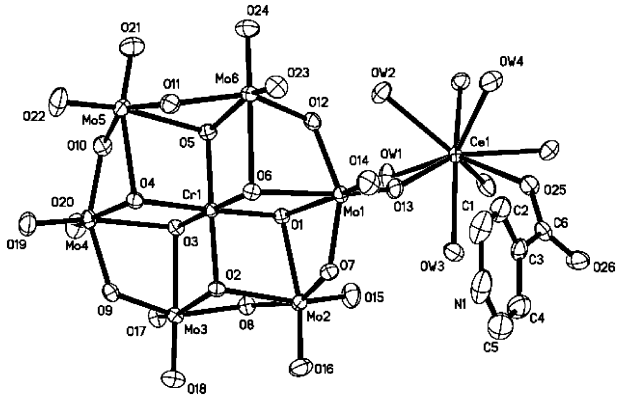

Fig. 1 ORTEP drawing of compound **1** with thermal ellipsoids at 50% probability level, free organic molecules and non-coordinated water molecules are omitted for clarity.

and Mo–Oc 2.248–2.331 Å in **2**; Mo–Ot 1.682–1.727, Mo–Ot′ 1.712–1.735, Mo–Ob 1.896–1.999 and Mo–Oc 2.248–2.337 Å in **3**; Mo–Ot 1.678–1.711, Mo–Ot′ 1.732–1.744, Mo–Ob 1.894–1.997 and Mo–Oc 2.241–2.325 Å in **4**. The central Cr–Oc distances vary from 1.958 to 1.986 Å in **1**, 1.965 to 1.994 Å in **2**, 1.965 Å to 2.000 Å in **3** and 1.957 to 1.997 Å in **4**. The O–Cr–O bond angles range from 83.4° to 178.5° in **1**, 83.3° to 178.5° in **2**, 83.2° to 178.4° in **3** and 84.2° to 178.2° in **4**, indicating that the $\{CrO_6\}$ octahedra are distorted to a similar extent in each case. There is only one crystallographically unique Ln(III) (Ln = Ce, Pr, La and Nd), residing in a distorted tricapped trigonal prism coordination environment in all four compounds, defined by two terminal oxygen atoms from two $[Cr(OH)_6Mo_6O_{18}]^{3-}$ units, three carboxyl oxygen atoms from two different pyridine-4-carboxylic acid molecules and four water molecules (as shown in Fig. 1 exemplifying the coordination environment of **1**). The average Ce–O bond length is 2.527 Å in **1**, Pr–O is 2.519 Å in **2**, La–O is 2.560 Å in **3**, and Nd–O is 2.501 Å in **4**. The variation of the Ln–O average bond distances along the La, Ce, Pr, Nd series (La–O > Ce–O > Pr–O > Nd–O) is consistent with the effect of lanthanide contraction due to the decrease of the ionic radius. The bond valence sum calculations indicate that the Cr, Ce, Pr, La and Nd sites are in the +3 oxidation state and all Mo sites are in the +6 oxidation state.[24]

The most remarkable feature in the four isostructural compounds is that the Anderson-type polyoxoanions are interlinked with each other *via* Ln^{3+} (Ln = Ce, Pr, La and Nd) ions to generate an unprecedented helical $[CrMo_6(OH)_6O_{18}Ln]_\infty$ chain, which possesses a 2_1 screw axis along the *b* axis (see Fig. 2). As shown in Fig. 3, adjacent same-handed helical chains are further interconnected by pyridine-4-carboxylic acid ligands to generate a 2D chiral layer with left-handed (L) or right-handed (R) helical chains in a ···L(R)···(pyridine-4-carboxylic acid)-L(R)··· mode (see also a space-filling view of the 2D chiral sheet based on the left-handed helices in **1** in Fig. S1 in the ESI). To our knowledge, no analogous 2D chiral layer framework, consisting of rare earth POM helical chains and organic bridging ligands, has been reported in the literature. Here, the pyridine-4-carboxylic acid ligands may be important for stabilizing the helices. In the 2D layer, there is one crystallographically independent pyridine-4-carboxylic acid molecule, which acts as a bidentate ligand by utilizing its carboxylate group to link two neighboring Ln^{3+}. As shown in Fig. 4 , the two types of chiral layers, one left-handed and the other right-handed, crystallize in pairs in the space group *C*2/*c* with an inversion center, leading to a mesomeric solid state compound.

Interestingly, the stacking of sheets indicates that hydrogen-bonding interactions exist between the adjacent layers such as the representative hydrogen bond O6–H6···O11 of 2.808 Å in

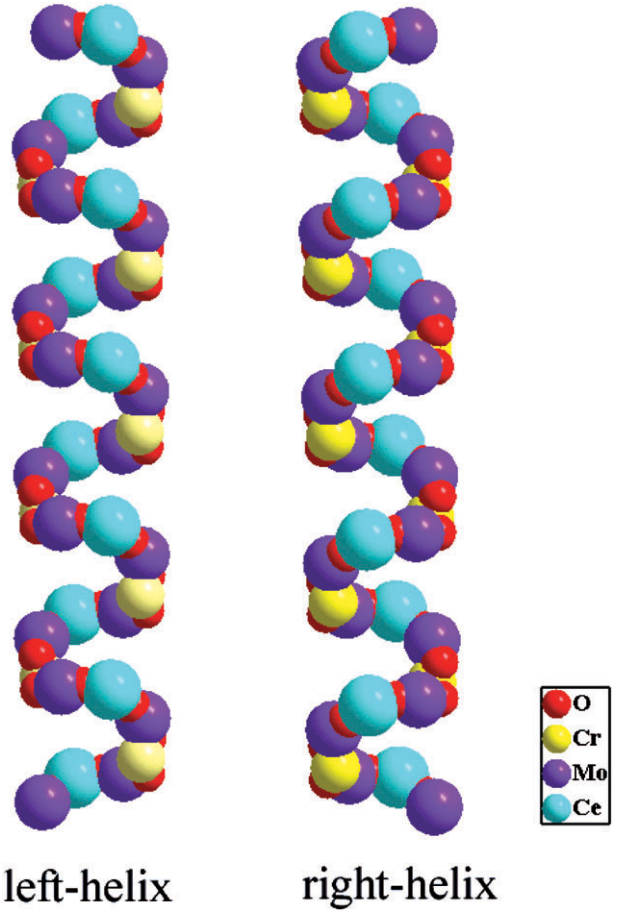

Fig. 2 Space-filling view of the left-handed and right-handed helical chains along the *b* axis exhibited by **1** (color code: Cr, yellow; Mo, purple; Ce, sky blue; O, red).

1 (see typical hydrogen bond distances in Table S2 in the ESI). It is obvious that hydrogen-bonding interactions between the polyoxoanions stabilize the packing of the neighboring layers. As a result, compounds **1–4** crystallize with an inversion center to form centrosymmetric solids, leading to the occurrence of the meso form of the compounds. Lattice water molecules, coordinated water molecules and free organic ligands also participate in the extensive hydrogen-bonding interactions and aide in stabilizing the chiral layer structure (see Table S2 in the ESI).

FT-IR spectra and TG analyses

In the IR spectrum of compound **1**, the features at 3614, 3409, 1638, 1590, 1578, 1398 and 1224 cm^{-1} can be regarded as characteristic bands of the pyridine-4-carboxylic acid molecule. The peaks at 939, 897, 853, 770, 642, 566 and 410 cm^{-1} are attributed to ν(Mo–Ot), ν(Mo–Ob) and ν(Mo–Oc) of the

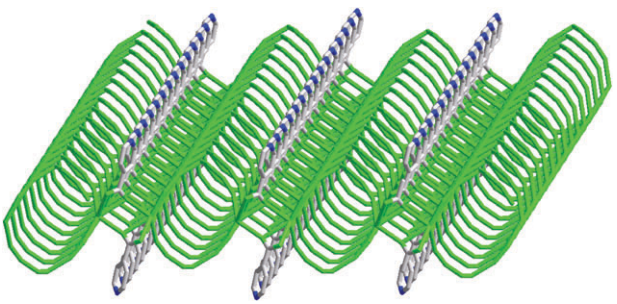

Fig. 3 Schematic view of the 2D chiral sheet based on the left-handed helices with the carboxyl oxygen atoms of the ligands as linkers in **1**.

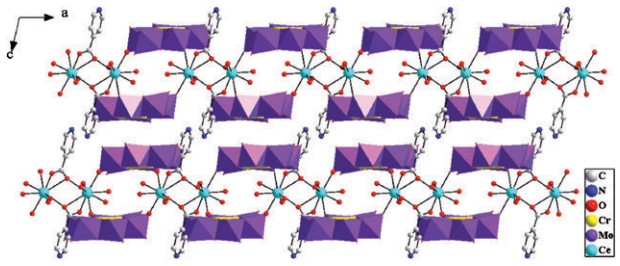

Fig. 4 View of the packing of **1** along the *b* axis, showing the two types of chiral layers in **1**, one left-handed and the other right-handed (color code: Cr, yellow; Mo, purple; Ce, sky blue; O, red; N, oxford blue; C, grey).

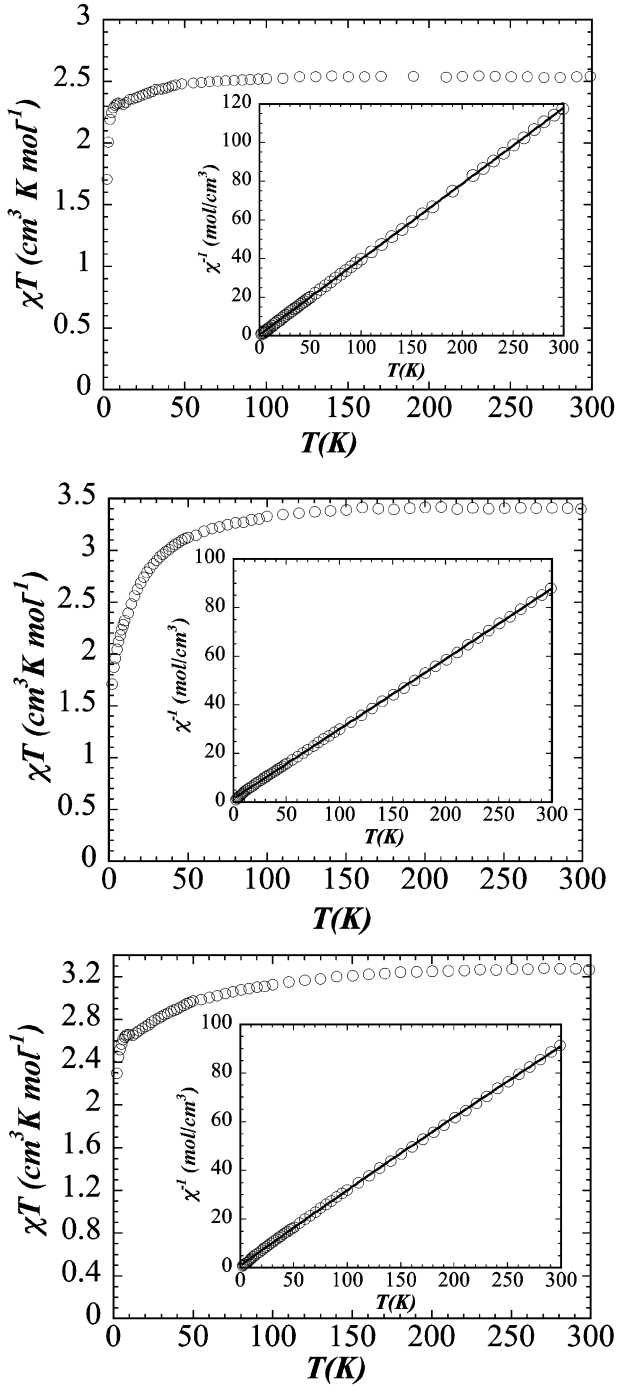

Fig. 5 The temperature dependence of reciprocal magnetic susceptibility χ_M^{-1} (inset) and the product $\chi_M T$ for compounds **1** (top), **2** (middle) and **4** (bottom).

$[Cr(OH)_6Mo_6O_{18}]^{3-}$ polyoxoanion. The IR spectra of compounds **2**, **3** and **4** are similar to that of **1** (see Fig. S3a–d in the ESI).

The thermal gravimetric (TG) curve of **1** is shown in as Fig. S4a in the ESI. It shows a total weight loss of 28.54% in the range of 50–700 °C, which agrees with the calculated value of 28.68%. The weight loss of 12.95% at 50–315 °C corresponds to the loss of all non-coordinated and coordinated water molecules (calcd 12.79%). The weight loss of 15.59% at 335–590 °C arises from the decomposition of organic molecules (calcd 15.89%). The TG curves of compounds **2**, **3** and **4** exhibit similar weight loss stages to those observed for compound **1** (see Fig. S4b–d in the ESI). The overall weight losses (28.96%, 28.49%, 28.94% for **2**, **3** and **4**, respectively) are in agreement with the calculated values (28.66%, 28.70%, 28.61% respectively), considering the loss of all water and the decomposition of the organic moieties..

Magnetic properties of compounds 1, 2 and 4

The magnetic susceptibilities of **1**, **2** and **4** were investigated from 300 to 2 K at 1 T on the polycrystalline samples (Fig. 5). When decreasing the temperature, the $\chi_M T$ of **1**, **2** and **4** decreases gradually from 2.51, 3.40 and 3.27 cm^3 K mol^{-1} at 300 K to reach 1.71, 1.70 and 2.29 cm^3 K mol^{-1} at 2 K, respectively. This behavior is typically observed for paramagnetic systems that exhibit dominating antiferromagnetic interactions. Curve fits for $1/\chi_M$ *versus* *T* plots of **1**, **2** and **4** with the Curie–Weiss law in the whole range of 2.0–300.0 K give good results with $C = 2.56$ cm^3 K mol^{-1} and $\theta = -1.34$ K for **1**, $C = 3.51$ cm^3 K mol^{-1} and $\theta = -5.3$ K for **2**, and $C = 3.18$ cm^3 K mol^{-1} and $\theta = -2.93$ K for **4**. Further analyses of the magnetic data will be carried out later when suitable models are found to fit the data.

Conclusions

In summary, we have synthesized the only structurally characterized rare earth POM complexes to date, featuring chiral and helical characters, by choosing a suitable POM building block and structure-directing agent. The successful isolation of the solid materials **1–4** provides not only novel examples of helical hybrid compounds, but also a new strategy for the design of polyoxoanion-based inorganic-organic hybrid materials containing helical or chiral structures. The pyridine-4-carboxylic acid molecule, acting as an organic ligand and a structure-directing agent, is certainly responsible for the formation of such a chiral framework with helical chains. The magnetic properties of **1**, **2** and **4** have been studied, which exhibit the antiferromagnetic interactions.

Acknowledgements

The authors thank the National Natural Science Foundation of China (20371011) for financial support.

References

1 (*a*) A. Müller, H. Reuter and S. Dillinger, *Angew. Chem., Int. Ed. Engl.*, 1995, **34**, 2328; (*b*) M. T. Pope and A. Müller, *Angew. Chem., Int. Ed. Engl.*, 1991, **30**, 34; (*c*) D. Hagrman, R. C. Haushalter and J. Zubieta, *Chem. Mater.*, 1998, **10**, 361.

2 (*a*) O. M. Yaghi, *Nature (London)*, 1999, **402**, 276; (*b*) O. M. Yaghi, *J. Am. Chem. Soc.*, 1998, **120**, 8571; (*c*) S. L. Zheng, J. H. Yang, X. L. Yu, X. M. Chen and W. T. Wong, *Inorg. Chem.*, 2004, **43**, 830; (*d*) B. Q. Ma, D. S. Zhang, S. Gao, T. Z. Jin, C. H. Yan and G. X. Xu, *Angew. Chem., Int. Ed.*, 2000, **39**, 3644; (*e*) M. Sasa, K. Tanaka, X. H. Bu, M. Shiro and M. Shionoya, *J. Am. Chem. Soc.*, 2001, **123**, 10750; (*f*) M. Du, Y. M. Guo, X. H. Bu, J. Ribas and M. Monfort, *New. J. Chem.*, 2002, **26**, 939.

3 (*a*) L. J. Prins, J. Huskens, F. D. Jong and P. Timmerman, *Nature (London)*, 1999, **398**, 498; (*b*) J. Chin, S. S. Lee, K. J. Lee, S. Park and D. H. Kim, *Nature (London)*, 1999, **401**, 254;

(*c*) H. Engelkamp, S. Middelbeek and R. J. M. Nolte, *Science*, 1999, **284**, 785; (*d*) J. Liang, Y. Wang, J. H. Yu and R. R. Xu, *Chem. Commun*., 2003, 882.
4 (*a*) X. M. Chen and G. F. Liu, *Chem.-Eur. J*., 2002, **8**, 4811; (*b*) J. Tao, J. X. Shi, M. L. Tong, X. X. Zhang and X. M. Chen, *Inorg. Chem*., 2001, **40**, 6328; (*c*) C. D. Wu, C. Z. Lu, X. Lin, D. M. Wu, S. F. Lu, H. H. Zhuang and J. S. Huang, *Chem. Commun*., 2003, 1284; (*d*) Z. R. Qu, H. Zhao, Y. P. Wang, X. S. Wang, Q. Ye, Y. H. Li, R. G. Xiong, B. F. Abrahams, Z. G. Liu, Z. L. Xue and X. Z. You, *Chem.-Eur. J*., 2004, **10**, 53.
5 (*a*) X. H. Bu, W. Chen, M. Du, K. Biradha, W. Z. Wang and R. H. Zhang, *Inorg. Chem*., 2002, **41**, 437; (*b*) X. H. Bu, H. Liu, M. Du, L. Zhang, Y. M. Guo, M. Shionoya and J. Ribas, *Inorg. Chem*., 2002, **41**, 5634; (*c*) P. A. Marggard, C. L. Stern and L. R. Poeppelmeier, *J. Am. Chem. Soc*., 2001, **123**, 7742; (*d*) R. Vaidhyanathan, S. Natarajan and C. N. R. Rao, *J. Solid State Chem*., 2004, **177**, 1444.
6 V. Soghomonian, Q. Chen, R. C. Haushalter, J. Zubieta and C. J. O'Connor, *Science*, 1993, **259**, 1596.
7 Z. Shi, S. Feng, S. Gao, L. Zhang, G. Yang and J. Hua, *Angew. Chem., Int. Ed*., 2000, **39**, 3243.
8 S. Neeraj, S. Natarajan and C. N. R. Rao, *Chem. Commun*., 1999, 165.
9 L. Xu, C. Qin, X. L. Wang, Y. G. Wei and E. B. Wang, *Inorg. Chem*., 2003, **42**, 7342.
10 (*a*) M. T. Pope, *Heteropoly and Isopoly Oxometalates*, Springer, Berlin, 1983; (*b*) C. L. Hill, *Chem. Rev*., 1998, **98**, 1; (*c*) S. Bareyt, S. Piligkos, B. Hasenknopf, P. Gouzerh, E. Lacôte, S. Thorimbert and M. Malacria, *Angew. Chem., Int. Ed*., 2003, **42**, 3404.
11 (*a*) U. Kortz, S. S. Hamzeh and N. A. Nasser, *Chem.-Eur. J*., 2003, **9**, 2945; (*b*) U. Kortz, M. G. Savelieff, B. S. Bassil, B. Keita and L. Nadjo, *Inorg. Chem*., 2002, **41**, 783; (*c*) E. Coronado, J. R. Galán-Mascarós, C. Giménez-Saiz, C. J. Gómez-García and S. Triki, *J. Am. Chem. Soc*., 1998, **120**, 4671.
12 P. J. Hagrman, D. Hagrman and J. Zubieta, *Angew. Chem., Int. Ed*., 1999, **38**, 2638.
13 (*a*) M. I. Khan, E. Yohannes and D. Powell, *Chem. Commun*., 1999, 23; (*b*) M. I. Khan, E. Yohannes and R. J. Doedens, *Angew. Chem., Int. Ed*., 1999, **38**, 1292.
14 (*a*) B. Z. Lin and S. X. Liu, *Chem. Commun*., 2002, 2126; (*b*) Y. G. Li, N. Hao, E. B. Wang, M. Yuan, C. W. Hu, N. H. Hu and H. Q. Jia, *Inorg. Chem*., 2003, **42**, 2729; (*c*) M. Yuan, Y. G. Li, E. B. Wang, Y. Lu, C. W. Hu, N. H. Hu and H. Q. Jia, *J. Chem. Soc., Dalton Trans*., 2002, 2916.
15 (*a*) A. Dolbecq, P. Mialane, L. Lisnard, J. Marrot and F. Sécheresse, *Chem.-Eur. J*., 2003, **9**, 2914; (*b*) J. Y. Niu, M. L. Wei, J. P. Wang and D. B. Dang, *Eur. J. Inorg. Chem*., 2004, 160; (*c*) J. Y. Niu, D. J. Guo, J. W. Zhao and J. P. Wang, *New. J. Chem*., 2004, **28**, 980.
16 (*a*) K. Fukaya and T. Yamase, *Angew. Chem., Int. Ed*., 2003, **42**, 654; (*b*) C. D. Wu, C. Z. Lu, H. H. Zhuang and J. S. Huang, *J. Am. Chem. Soc*., 2002, **124**, 3836; (*c*) J. J. Zhang, T. L. Sheng, S. Q. Xia, G. Leibeling, F. Meyer, S. M. Hu, R. B. Fu, S. C. Xiang and X. T. Wu, *Inorg. Chem*., 2004, **43**, 5472; (*d*) C. B. Liu, C. Y. Sun, L. P. Jin and S. Z. Lu, *New. J. Chem*., 2004, **28**, 1019; (*e*) J. R. Li, X. H. Bu, R. H. Zhang, C. Y. Duan, K. M. C. Wong and V. W. W. Yam, *New J. Chem*., 2004, **28**, 261.
17 H. Y. An, Y. Lan, Y. G. Li, E. B. Wang, N. Hao, D. R. Xiao, L. Y. Duan and L. Xu, *Inorg. Chem. Commun*., 2004, **7**, 356.
18 (*a*) V. Shivaiah, P. V. N. Reddy, L. Cronin and S. K. Das, *J. Chem. Soc., Dalton Trans*., 2002, 3781; (*b*) D. Drewes, E. M. Limanski and B. Krebs, *J. Chem. Soc., Dalton Trans*., 2004, 2087.
19 H. Y. An, Y. Q. Guo, Y. G. Li, E. B. Wang, J. Lü, L. Xu and C. W. Hu, *Inorg. Chem. Commun*., 2004, **7**, 521.
20 C. Qin, L. Xu, Y. G. Wei, X. L. Wang and F. Y. Li, *Inorg. Chem*., 2003, **42**, 3107.
21 A. Perloff, *Inorg. Chem*., 1970, **9**, 2228.
22 (*a*) B. J. Kennedy and K. Murray, *Inorg. Chem*., 1985, **24**, 1552; (*b*) E. A. Boudreaux and L. N. Mulay, *Theory and Applications of Molecular Paramagnetism*, John Wiley and Sons, New York, 1976, p. 491.
23 (*a*) G. M. Sheldrick, *SHELXL-97, Program for refinement of crystal structures*, University of Göttingen, Germany, 1997; (*b*) G. M. Sheldrick, *SHELXS-97, Program for solution of crystal structures*, University of Göttingen, Germany, 1997.
24 I. D. Brown and D. Altermatt, *Acta Crystallogr., Sect. B*, 1985, **41**, 244.